Astron. Astrophys. 326, 271–276 (1997)

ASTRONOMY
AND
ASTROPHYSICS

Mid infrared spectral observations of UX Orionis⋆

H.-G. Reimann[1], **J. Gürtler**[1], **C. Friedemann**[1], **and H. U. Käufl**[2]

[1] Friedrich-Schiller-Universität Jena, Astrophysikalisches Institut und Universitäts-Sternwarte, Schillergäßchen 2, D-07745 Jena, Germany
[2] European Southern Observatory, D-85748 Garching, Germany

Received 21 October 1996 / Accepted 25 April 1997

Abstract. The circumstellar infrared emission of the evolutionarily young irregular variable UX Orionis has been investigated. The observed spectral energy distribution has been modelled by radiative transfer calculations and the parameters for a spherically symmetric envelope have been derived. Two mid-infrared spectra of UX Orionis were obtained with the **T**hermal **I**nfrared **M**ulti**m**ode **I**nstrument (TIMMI) at the ESO 3.6-m telescope. The spectra show the presence of a nearly structureless silicate emission band. Comparison with laboratory data indicates that the circumstellar silicate grains should have radii of $a \approx 0.75$–1 μm.

Key words: stars: individual: UX Ori – stars: circumstellar matter – (ISM:) dust, extinction – infrared: stars

1. Introduction

The irregular variable UX Orionis (= BD −4 1029 = HD 293782 = IRAS 05020−0351) belongs to the evolutionarily young stars of the Orion population (Herbig & Bell 1988). It is, however, not a typical member of Herbig Ae/Be stars as it is not associated with a nebulosity.

UX Ori belongs to a subclass of irregular variables originally suggested by Hoffmeister (1949). More recently, UX Ori is often considered as the prototype of this subclass (Voshchinnikov 1989, Herbst et al. 1994). Its light curve seems to consist of several components. In addition to long-term wave-like variations, there are irregularly occurring short-lasting deep Algol-like minima.

Discussing UBV measurements of SV Cep, another member of this subclass, Wenzel (1969) suggested occultations by circumstellar dust clouds as a reason for the Algol-like minima. This hypothesis was subsequently further developed by many authors (Wenzel et al. 1971; Gahm et al. 1974; Zaytseva & Chugainov 1984; Voshchinnikov 1989; Grinin et al. 1991; Graham 1992; Friedemann et al. 1992, 1993, 1995, Herbst et al. 1994) and got increasing acceptance. The detection of infrared excesses by IRAS confirmed the presence of circumstellar dust and led to the construction of quantitative models of circumstellar dust shells.

UX Ori has been studied intensively in recent years. It is associated with the IRAS point source 05020−0351. The infrared radiation of the circumstellar dust shell was modelled by Bibo & Thé (1990), Hillenbrandt et al. (1992), and Hartmann et al. (1993). Grinin et al. (1994) discussed photometric, polarimetric and spectroscopic observations of a very deep minimum in some detail.

In this paper we will present the first infrared spectrum of the circumstellar dust in the wavelength region 8–13 μm. The spectrum is compared with laboratory data of silicate dust. The physical conditions within the circumstellar shell are estimated by means of a spherically symmetric model providing an acceptable fit of the observed spectral energy distribution.

2. Observations and data reduction

The data were recorded during the commissioning of the grism mode of the ESO mid-infrared camera TIMMI (**T**hermal **I**nfrared **M**ulti**m**ode **I**nstrument) at the 3.6-m telescope in December 1995. Using the spectroscopy mode of this instrument, we obtained 10 μm spectra of UX Ori . We used three grisms covering the wavelength ranges from 7.8 μm to 9.4 μm, 9.3 μm to 11.2 μm, and 10.9 μm to 13.3 μm, respectively. The spectral resolution is not exactly the same for the different grisms. It varies from 0.026 μm/pixel for the 8 μm grism to 0.037 μm/pixel for the 12 μm grism. The wavelength calibration was done in the laboratory by scanning black body radiation with a monochromator. A more detailed technical description of TIMMI was given by Käufl (1994) and Käufl et al. (1994).

In the two nights of December 5 and 6 we obtained two complete spectra (that means two sets of three single spectra according to the different grisms) of UX Ori with a signal-to-noise ratio $S/N \approx 4$. In the first night we observed comparison spectra of α Car before and after the exposures for UX Ori. In the second night we obtained spectra of α Car before and of α CMa after the exposures for UX Ori at nearly the same airmass. The

Send offprint requests to: H.-G. Reimann

⋆ Based on observations collected at the European Southern Observatory, La Silla, Chile.

signal-to-noise ratio of the spectra of the comparison stars was $S/N \approx 20$. Typical integration times for one grism including all copping and nodding cycles were 30 min for UX Ori and 5 min in case of a comparison star.

The wavelength calibration was checked by comparing the peaks in the observed atmospheric transmission curve with the positions of the atmospheric absorption lines (especially O_3 around 9.8 μm). However, we cannot completely exclude a remaining wavelength calibration error in the order of one pixel ($\Delta\lambda \approx 0.031$ μm). This residual error is due to the limited mechanical accuracy to set the aperture wheel of the camera containing the slits to a given position.

Comparing the two standard stars in each of the two nights during the process of data reduction, it turned out that the atmospheric extinction must have varied rapidly during these two nights because the differences between these spectra could not be accounted for by the different airmasses alone. The deviations reach up to 10 per cent at some wavelengths. Because of this fact we reduced the data in two different ways. First, we used the spectra of the comparison stars to derive the atmospheric transmission and to reduce the programme star spectra and, second, we used model calculations of the atmospheric transmission to obtain the spectra for UX Ori.

As one way to reduce our data we derived the atmospheric transmission by comparing our spectra of α Car and α CMa with their IRAS LRS spectra (IRAS Science Team 1986). Both IRAS spectra are featureless Rayleigh-Jeans-type spectra of class 18 with a $S/N \approx 25$. For the reduction of the TIMMI spectra we interpolated the IRAS spectra for the corresponding pixel wavelengths. In the case of α CMa we compared the IRAS spectrum also with the calibrated model spectrum of α CMa by Cohen et al. (1992). We found a flux ratio of 0.945 of the model spectrum to the LRS spectrum. This could imply that our fluxes of UX Ori that are based on the IRAS spectra are too large by about 5 per cent. In the reduction procedure for the three wavelength intervals (corresponding to the three grisms), we always used the comparison spectrum that had the shortest time difference from the UX Ori exposures. This time difference was at maximum two hours. The angular difference on the sky between UX Ori and the comparison stars was 25° and 50° for α Car and α CMa, resp. The resulting differences in airmass X were in no case larger than $\Delta X = 0.20$. After the reduction the three parts of the spectra fit well together. The mean of the two spectra of UX Ori is presented in the upper panel of Fig. 1. The good agreement can clearly be seen in the overlapping region between the 10 μm grism and the 12 μm grism around 11 μm. The lower panel of Fig. 1 shows the combined effect of atmospheric extinction and sensitivity of the IR-array. The observational error is approximately inversely proportional to the signal. It is obvious that the noise increases considerably towards both atmospheric cut-offs and at the position of the O_3 absorption band.

As a second reduction procedure we used the atmospheric transmission model by Wooden (1996, priv. comm.) to remove

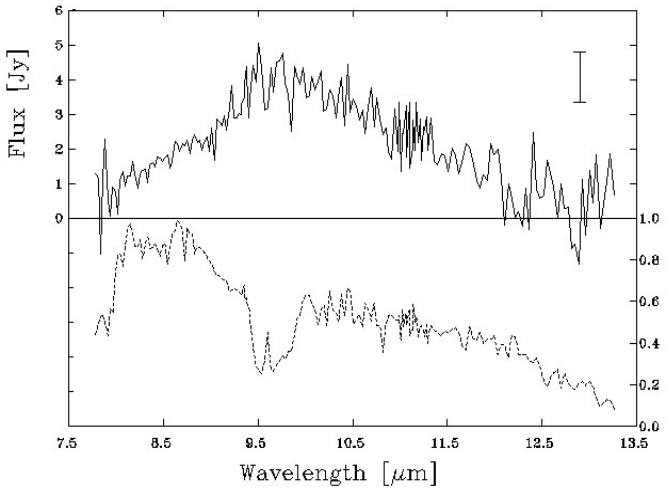

Fig. 1. The combined spectrum of UX Orionis covering the whole 10 μm atmospheric window from 7.8 μm to 13.3 μm (upper panel). The noise increases considerably towards both of the atmospheric cut-offs and within the O_3 absorption band. The lower panel represents the combined effect of atmospheric extinction and sensitivity of the IR-array derived from the flux ratio of the comparison spectra. The slope in the lower curve is due to the decreasing sensitivity of the chip towards the longer wavelengths. The dip around 9.8 μm is due to telluric O_3 not fully compensated for because of its time variation. The bar indicates the mean error typical of the 10 μm region.

the effects of the atmosphere. We calculated the atmospheric transmission $T(\lambda, X)$ for the airmass X using the formula

$$T(\lambda, X) = \exp(-b(\lambda) \cdot \sqrt{X} - c(\lambda) \cdot X), \quad (1)$$

where $b(\lambda)$ and $c(\lambda)$ are functions given by the model. For fine-tuning we varied the airmass until we got the best fit to the ratio of the IRAS spectra and the observed spectra of α Car and α CMa. The result is virtually the same as that shown in Fig. 1. However, it turned out that, as in the first procedure, the influence of the atmosphere could not be fully removed by adjusting the transmission model by the airmass at the time of observation alone. During the whole sequence of observations the amount of water vapour and ozone must have changed.

3. Modelling of the circumstellar dust shell

3.1. Available optical and infrared data

For UX Orionis many photometric data exist. They show irregular light variations in the optical wavelength region. Algol-like minima with amplitudes up to $\Delta V \approx 2.5$ mag are the most prominent among these variations and indicate that the star is obscured from time to time by circumstellar dust clouds. The presence of circumstellar dust is convincingly revealed by the infrared data. Measurements in the K band show some degree of variability (see, e. g., Kolotilov et al. 1977). The observed amplitude is, however, compatible with a constant envelope contribution. Our modelling (see below) predicts that 30–40 per cent of

the total light at K comes from the star. Therefore, the obscuration of the star by a circumstellar cloud must have observational consequences at K. However, some fraction of the variability may also arise from star spots since Evans et al. (1989) gave evidence for variations of the effective temperature of the star. The IRAS data are compatible with the notion of a constant shell luminosity. The probability of variable IRAS fluxes is 20 per cent.

The spectral type of UX Ori is A3e III after Herbig & Bell (1988), while Tjin A Djie et al. (1984) classified it as A2 III. Therefore, we adopt a luminosity of 53 $L_\odot$ and an effective temperature of 8600 K in our model calculations.

The interstellar extinction in the direction to UX Ori is only poorly known because it is situated at the high galactic latitude of $b \approx -25°$ and only few photometric data of early-type field stars are available. Fitzgerald (1968) gives $E(B-V) \leq 0.1$ mag for distances $r \lesssim 500$ pc. Walker (1969) determined $E(B-V) = 0.06$ as the foreground extinction of the Orion Complex. Observational data obtained for UX Ori by different authors (Zaytseva 1973; Herbst et al. 1983; Tjin A Djie et al. 1984) give colour indices $B-V$ = 0.28–0.38 outside Algol-like minima. We consider $B-V = 0.33$ as a typical value. Adopting an intrinsic colour index of $(B-V)_0 = 0.06$ (Schmidt-Kaler 1982), we find a colour excess of $E(B-V) = 0.27$. If UX Ori has the same foreground extinction as the Orion Complex, the circumstellar shell produces a reddening of $E(B-V)_{\rm circ} = 0.21$ outside the Algol-like minima. Therefore, the circumstellar shell must consist of a diffuse more or less smoothly distributed component and a second that is formed by a larger number of clouds responsible for the stellar occultations we observe as Algol-like minima.

3.2. A spherically symmetric circumstellar shell

In order to get some information about mass and extent of the circumstellar dust distribution, we adopt a simple spherically symmetric model. In our modelling we will assume that the obscuring of the star by the dust clouds does not strongly influence the temperature structure, and consequently the emission of the shell is invariable. We use the brightness measurements of the star during maximum light as representative for the irradiation of the circumstellar dust. The effect of the clumpiness on the emission of the shell should be small since the observed infrared radiation comes from the whole shell and the clumps are optically thin at IR wavelengths.

The calculations were done using a code which is discussed in some detail by Chini et al. (1986). Input parameters of the computer program are the radius of the inner dust free zone, the outer radius of the envelope, and the radial dust density distribution (approximated by a power law). The star as the central heating source is characterized by its luminosity and effective temperature. For the optical properties of the dust grains we used the data published by Draine & Lee (1984). The relative proportions of the silicate and carbon is set by the condition that there are per H atom 3×10^{-4} C atoms in graphite and 3.1×10^{-5} Si atoms in silicate.

Table 1. Model parameters for a spherically symmetric circumstellar dust shell around UX Ori

Spectral type	A3e III
Effective temperature (K)	8600
Luminosity ($L_\odot$)	53
Distance (pc)	550
$E(B-V)_{\rm circ}$ (mag)	0.21
Boundaries of the shell	
$r_{\rm i}$ (a.u.)	2.7
$r_{\rm o}$ (a.u.)	2270
Density distribution	$r^{-1.22}$
Total mass of circumstellar dust ($M_\odot$)	$6.2\ 10^{-6}$
Dust temperatures	
$T_{\rm sil}(r_{\rm i})$ (K)	900
$T_{\rm sil}(r_{\rm o})$ (K)	40
$T_{\rm C}(r_{\rm i})$ (K)	1200
$T_{\rm C}(r_{\rm o})$ (K)	60

In Fig. 2 we compare the result of our model calculations with the observed spectral energy distribution (SED). The parameters of the fit are listed in Table 1. Keeping in mind the simplifying assumtions on witch our modelling is based, we did not attempt to select our final model by a χ^2-test but only by a visual judgement of the quality of the fit. In the fitting procedure we attempted to reproduce the SED defined by maximum brightness since the obscuration of the star should not effect the heating of the envelope. The general trend of the SED is well represented. However, there is a discrepancy in the 3–8 μm region. All our attempts to get a better fit in this spectral range failed. We conclude from this fact that for this shape of the SED the simple model of a smooth density distribution is not fully appropriate. Bibo & Thé (1990) reproduced the SED by assuming two distinct isothermal shells, which is certainly an oversimplification.

It is noteworthy that the dip in the spectrum of UX Ori at 4.8 μm in the SED is not unique among Herbig Ae/Be stars but can be seen in the spectra of a relatively large number of objects (see Hartmann et al. 1993, Hillenbrand et al. 1992). It seems unlikely that it due to the observational uncertainties alone although it cannot excluded that the time-dependent influence of some constituents of the earth's atmosphere (O_3, CO_2, H_2O) could not be removed completely. The modelling of the dip at 4.8 μm lies beyond the scope of this paper. Since our model calculations reproduce the general trend of the SED, we feel that the results for the density and temperature distributions of the circumstellar dust grains are a realistic basis for the modelling of the observed profile of the 10 μm emission band (see Sect. 4.).

Our model predicts a far too low 100 μm flux if compared with the IRAS observations. However, this value is probably contaminated by cirrus emission and therefore uncertain.

The assumption of spherical symmetry is certainly a great simplification. There is much evidence for disk-like structures around young stars. The orbital motion of the clouds causing the Algol-like minima may point to a proto-planetary system.

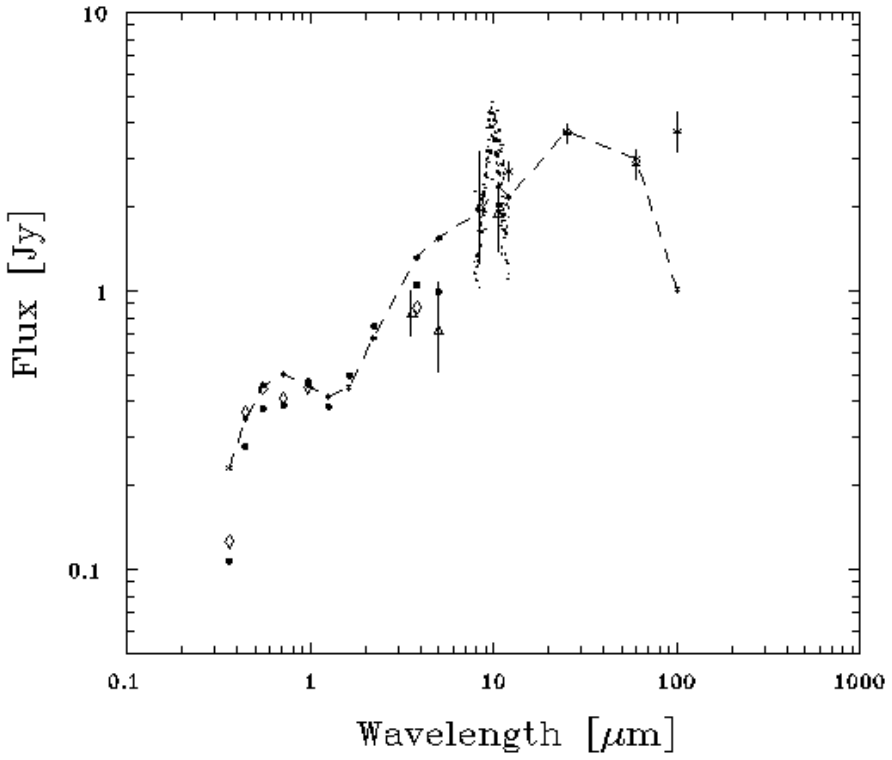

Fig. 2. The observed spectral energy distribution of UX Ori and the prediction of our spherically symmetric model. The observations are from Herbst et al. (1983) ◇, Cohen (1973) △, IRAS ×, and Hillenbrand et al. (1992) •. The vertical bars indicate observational errors. Our observed 10 μm spectrum is shown too.

Our modelling of the infrared radiation shows that the envelope is much more extended than the region where the occulting clouds move (see Friedemann et al. 1995). It seems plausible that the outer parts of the circumstellar shell kept their spherical symmetry. Moreover, the small optical depth of the circumstellar dust shell secure that all circumstellar dust grains contribute to the observed infrared radiation. Therefore, the estimate of the total dust mass is not sensitive to the exact geometry of the shell. Actual deviations from the spherical symmetry would influence the shape of the density distribution.

It seems remarkable that the density distribution in the circumstellar shells of the Herbig Ae/Be stars UX Ori, SV Cep, WW Vul modelled by us (this paper, Friedemann et al. 1992, 1993) deviates significantly from a r^{-2} law . Recently Miroshnichenko et al. (1977) reached a comparable result for 9 additional stars.

4. Modelling of the 10-μm silicate emission band

The observed spectrum shown in Fig. 1 exhibits the 10 μm silicate band in emission. The relatively large scatter of the data points makes it impossible to discern any structure if present in the band.

Observations of the silicate feature in the spectra of T Tauri stars and Herbig Ae/Be stars have been reported by Cohen (1980), Cohen & Witteborn (1985), and Hanner et al. (1995). The silicate band is seen as an emission feature in several objects, but also as an absorption band in others. Our profile of UX Ori matches the shape of the mean emission feature derived by Cohen (1980) from 5 T Tauri stars quite well. Contrary to this, the profile of Elias 1 derived by Hanner et al. (1994) is very different from our profile. It is much broader and the flat profile has its maximum beyond 10.5 μm.

Determining the spectral emissivity of the silicates from observations requires the knowledge of the optical depths and the temperatures of the dust components contributing to the observed fluxes in the 10 μm region. The lack of such knowledge led to the construction of simple models in the past (Gillett et al. 1975, Cohen & Witteborn 1985). The basic result of this procedure is that the observed profiles can be reproduced if the silicates are assumed to emit like the silicates in the Orion Trapezium region. The validity of the model parameters is limited by the fact that the spectral region used in the fitting procedure is small compared with the whole wavelength region dominated by the dust emission.

Our observational data for UX Ori can be easily explained in the frame of the mentioned simple models. For instance, using the isothermal model by Cohen & Witteborn (1985) and adopting a power law for the source function instead of a Planck function, (see i.e. Hanner et al. 1995)

$$F_\nu = a_0 \cdot (\nu/\nu_0)^n \cdot (1 - \exp(-a_1 \cdot \epsilon_\nu)), \quad (2)$$

where ϵ_ν is the emissivity of the Orion Trapezium dust, we find as parameters $a_0 = 15 \pm 2$, $a_1 = 0.3 \pm 0.03$, $n = 1 \pm 0.2$. The general slope of the dust emission in the 10 μm region is, however, characterized rather by $\nu^{-2/3}$ (see Fig. 2). This discrepancy shows that a fitting based on a small portion of the spectrum may lead to physically unrealistic results.

Consequently it seems appropriate to use the temperature and density distributions from the modelling of the overall SED

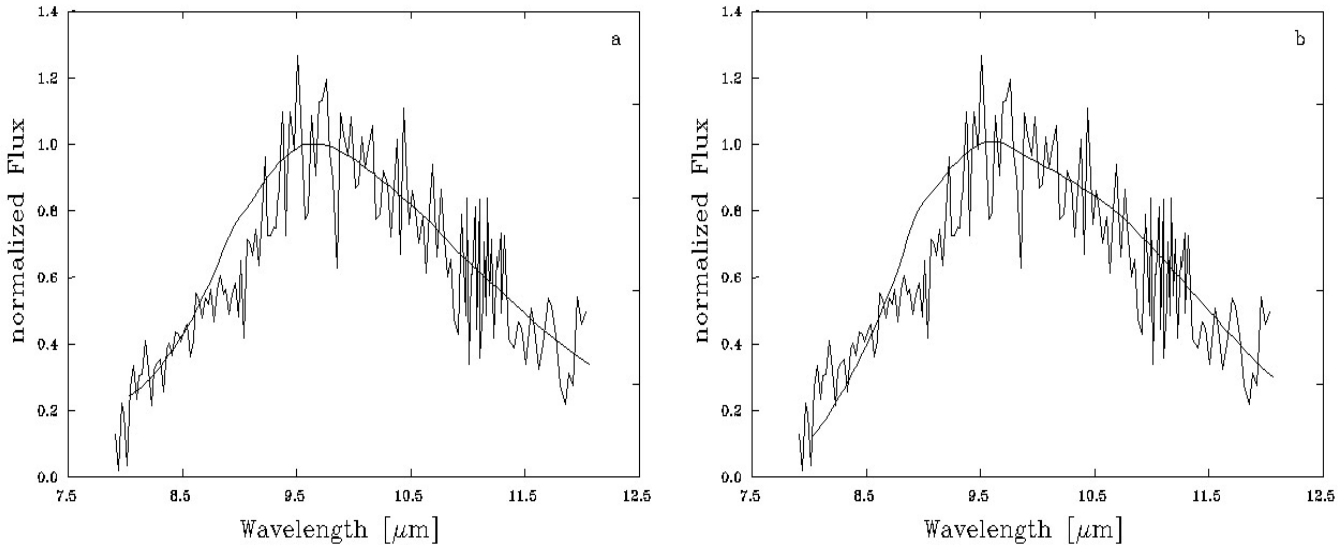

Fig. 3a and b. The observed 10 μ emission band in the spectrum of UX Orionis compared with calculations based on laboratory data of glassy silicates. **a** The observed spectrum and the calculated profile for a mixture of glassy pyroxene and olivine spheres (a = 0.75 μm). **b** The observed spectrum and Mie calculations for glassy pyroxene spheres with a grain radius of a = 1 μm.

(see Sect. 3.2.) as a starting point to calculate the emission of the silicate feature. Assuming again the emissivity of the Orion Trapezium silicate dust, the model predicts a strong excess on the long-wavelength side of the 10 μm band. (It is just this excess that is avoided by a source function $\propto \nu$ in the model fitting procedure above!) We have to conclude that the silicate dust around UX Ori (and probably around other T Tauri stars, too) emits less strongly on the long-wavelength side of the 10 μm peak than the Orion Trapezium dust.

Another approach may consist of using laboratory data of astrophysically plausible silicates for the explanation of the observed 10 μm emission band. Cosmic abundances, conditions of grain formation in circumstellar envelopes, and interstellar elemental depletions all point to Mg-Fe silicates as the dominant interstellar silicate component and silicate glasses may be likely laboratory analogues of them (Dorschner & Henning 1986). Dorschner et al. (1995) published a thorough study of the optical constants of glassy olivines and pyroxenes of various Mg-Fe content. We used their data in our attempt to reproduce the UX Ori spectrum. In order to limit the parameters in the fitting procedure, we adopted their laboratory data for the silicates with an Mg/Fe ratio of 1. Additionally to the silicate emission, we assumed in the modelling that there is an underlying continuous emission from graphite as our spherically symmetric model predicts.

Because the observed profile peaks below 10 μm pyroxenes seem to be better suited than olivines. Figure. 3b shows the result of our calculations. The overall representation of the profile is acceptable but not fully satisfying. An acceptable fit of the long-wavelength part of the profile could be reached only by assuming rather large particle sizes (typical radii $a \approx 1$ μm).

The experience with the silicates in our Solar System shows that both pyroxenes and olivines exist. This notion led Pollack et al. (1994) to suggest a dust model in which - among other components - the silicate comes in a mixture of pyroxene and olivine in the ratio of 23:67. Several authors have successfully modelled the 10 μm band of a number of comets by a mixture of different silicates (Bregman et al. 1987; Colangeli et al. 1995, 1996). This motivated us to include mixtures of pyroxene and olivine in our considerations. Figure. 3a shows the result of our calculations. A somewhat better representation of the observed profile could be reached. This seems not very surprising as more free parameters were available. On the other hand, the discrepancy between 8.8 and 9.3 μm remains. The parameters of the fit are: pyroxene/olivine ratio (by grain number) 1:1, grain radius $a = 0.75\mu$m.

We wish to emphasize that our both fits of the 10 μm band with the laboratory data for glassy silicates requires grain radii significantly larger than those assumed in interstellar space. There is already some evidence that the circumstellar grains have larger sizes than interstellar ones (see, e. g., Chini et al. 1991; Mannings & Emerson 1994). Thus, the very broad 10 μm feature observed by us provides an additional argument for grain growth in the circumstellar environment.

5. Conclusions

1. The light variations of UX Ori show prominent Algol-like minima, which are caused by circumstellar dust clouds orbiting the star.
2. The IRAS data reveals an infrared dust emission originating from thermalized stellar radiation.
3. We performed radiative transfer calculations to derive the physical parameters of the circumstellar dust shell and found

that the density varies as $r^{-1.225}$ in good agreement with the distributions in the circumstellar shells of other Herbig Ae/Be stars.

4. Comparing the profile of the 10 μm silicate band with laboratory data for glassy Mg-Fe pyroxene and olivine indicates that the silicate consists of pyroxene or a mixture of pyroxene and olivine and the grains have diameters of about 0.75 to 1 μm.
5. The grain sizes needed to explain the observed profile fit nicely with other observations indicating that circumstellar grains are larger than the interstellar ones.

Acknowledgements. We thank our referee, Dr. J. Emerson, for valuable comments which improved our paper very much. Furthermore, we are indebted to Drs. J. Dorschner and H. Mutschke (Arbeitsgruppe "Staub in Sternentstehungsgebieten" of the Max-Planck-Gesellschaft at the Friedrich-Schiller-Universität) for valuable discussions and providing us with the optical data of olivine and pyroxene. This work was partially supported by Deutsche Forschungsgemeinschaft (Fr 963/3-1) and the German Bundesministerium für Bildung, Wissenschaft, Forschung und Technologie (Förderkennzeichen 05 3JN13A).

References

Bibo E.A., Thé P.S., 1990, A&A 236, 155
Bregman J. D., Campins H., Witteborn F. C., et al., 1987, A&A 187, 616
Chini R., Krügel E., Kreysa E., 1986, A&A 167, 315
Chini R., Krügel E., Shustov B., Tutukov A., Kreysa E., 1991, A&A 252, 220
Cohen M., 1973, MNRAS 161, 97
Cohen M., 1980, MNRAS 191, 499
Cohen M., Walker R.G., Barlow M.J., Deacon J.R., 1992, AJ 104, 1650
Cohen M., Witteborn F.C., 1985, ApJ 294, 345
Colangeli L., Mennella V., Palumbo P., Rotundi A., Bussoletti E., 1995, A&A 293, 927
Colangeli L., Mennella V., Rotundi A., Palumbo P., Bussoletti E., 1996, A&A 312, 643
Dorschner J., Henning Th.,1986, A&SS 128, 47
Dorschner J., Begemann B., Henning Th., Jäger C., Mutschke, H., 1995, A&A 300, 503
Draine B.T., Lee H.M., 1984, ApJ 285, 89
Evans A., Davies J.K., Kilkenny D., Bode M.F. 1989, MNRAS 237, 695
Fitzgerald M.P., 1968, AJ 78, 983
Friedemann C., Reimann H.-G., Gürtler J., 1992, A&A 255, 246
Friedemann C., Reimann H.-G., Gürtler J., Tóth V., 1993, A&A 277, 184
Friedemann C., Gürtler J., Reimann H.-G., 1995, A&A 300, 269
Gahm G. F., Nordh H. L., Olofsson N. C., Carlborg N. C. J., 1974, A&A 33, 399
Gillett F.C., Forrest W.J., Merrill K.M., Capps R.W., Soifer B.T., 1975, ApJ 200, 609
Graham J. R., 1992, PASP 104, 479
Grinin V. P., Kisilev N. N., Minikulov N. Kh., Chernova G. P., Voshchinnikov N. V., 1991, Ap&SS 186, 283
Grinin V.P., Thé P.S., de Winter D., et al., 1994, A&A 292, 165
Hanner M.S., Brooke, T.Y., Tokunaga A.T., 1994, ApJ 433, L95
Hanner M.S., Brooke, T.Y., Tokunaga A.T., 1995, ApJ 438, 250
Hartmann L., Kenyon S.J., Calvet N., 1993, ApJ 407. 219
Herbig G.H., Bell K.R., 1988, Lick Obs. Bull. No. 1117
Herbst W., Herbst D., Grossmann E., Weinstein D., 1994, AJ 108, 1906
Herbst W., Holtzman J.A., Klastey R.S., 1983, AJ 88, 1648
Hillenbrand L.A. , Strom S.E., Vrba F.J., Keene J., 1992, ApJ 397, 613
Hoffmeister C., 1949, Astron. Nachr. 278, 24
IRAS Science Team, 1986, A&AS 65, 607
Käufl H.U., 1994, The Messenger 78, 4
Käufl H.U., Jouan R., Lagage P.O., et al., 1994, Infrared Phys. Technol. 35, 302
Kolotilov E.A., Zaytseva G.V., Shenavrin V.I. 1977, Astrofiz. 13, 456
Mannings V., Emerson J. P., 1994, MNRAS 267, 361
Miroshnichenko A., Ivezić Ž., Elitzur M., 1997, ApJ 475, L41
Pollack J. B., Hollenbach D., Beckwith S., Simonelli D. P., Roush T., Fong W., 1994, ApJ 421, 615
Schmidt-Kaler Th., 1982, in: Landolt-Börnstein, Zahlenwerte und Funktionen aus Naturwissenschaften und Technik, Springer-Verlag, Berlin-Heidelberg-New York, NS, Gr. VI, Vol. 2b, p. 449
Tjin A Djie H. R. E., Remijn L., Thé P.S., 1984, A&A 134, 273
Voshchinnikov N. V., 1989, Astrofiz. 30, 509
Walker M., 1969, ApJ 155, 447
Wenzel W., 1969, Mitt. Veränderliche Sterne, Sonneberg, 5, 75
Wenzel W., Dorschner J., Friedemann C., 1971, Astron. Nachr. 292, 221
Zaytseva G.V., 1973, Perem. Zvezd. 19, 63
Zaytseva G. V., Chugainov P. F., 1984, Astrofiz. 20, 447

This article was processed by the author using Springer-Verlag LaTeX A&A style file *L-AA* version 3.